

Supplementary figure legend

Fig. S1A: VEGFR2 is differentially expressed on NSCLC

Cell lines H1650, A549, H1975, H441, HCC1359 and HUVECs were stained for VEGFR2 by flow cytometry. Briefly, 100,000 cells were fixed with 4% Formaldehyde for 20 min at 4 °C, permeabilized with 0.5% Saponin in PBS for 20 min at 4°C. Cells were stained with anti-VEGFR2-antibody (clone 55B11, 1:100, Cell Signaling) for 30 min at 4°C. Alexa-488 conjugated goat anti-rabbit antibody (A-11034, 1:1000, Life technologies) was used. Data from 10,000 cells per sample were acquired on a FACS Canto (BD Bioscience) and FlowJo (Tree Star) software was used for data analysis.

Fig. S1B: ZD6474 treatment does not affect tumor cell proliferation

H1975 and H441 were screened for identification of actively cycling cells as opposed to non-cycling cell fractions. 3×10^6 cells were plated in 6-well plates and incubated for 24 hours in starving media. Cells were then either treated with DMSO (D) or stimulated with 40ng VEGF (V) alone dissolved in DMSO (D+V) or in addition to pretreatment with the ZD6474 (0.5 and 1 μ M) (Z+V) for 4 hours. Bromo-deoxy-uridine (an analog of the DNA precursor thymidine) was incorporated into newly synthesized DNA by cells entering and progressing through the S (DNA synthesis) phase of the cell cycle. The incorporated BrdU was stained with specific anti-BrdU fluorescent antibodies. All protocols were performed according to BrdU Flow Kit from BD Pharmingen (cat. No. 559619). The levels of cell-associated BrdU were then measured on a Gallios flow cytometer from Beckman Coulter. Results were calculated using Gallios FACS software. Bars represent the percentage of proliferative (BrdU positive) cells under different treatment conditions.

Fig. S1C: ZD6474 treatment affects amino acid transport without hampering tumor cell proliferation

H1975 cells were engrafted subcutaneously in nude mice; mice with established tumors were treated with ZD6474 (75mg/kg daily by oral gavage) and MET/FLT imaging was performed on day 0 (before start of therapy) and at the indicated time points after treatment. Representative results are shown. Methionine uptake in the tumors was substantially reduced after 7days of treatment compared to FLT uptake, which showed a slight increase.

Fig. S1D: Reduction in MET uptake is specifically due to ZD6474 mediated VEGFR2 inhibition

Substitution of Val916 by Met at the gatekeeper position of VEGFR2 creates a steric clash with the inhibitor and prevents ZD6474 from binding to the VEGFR2 binding pocket. The introduction of this resistant gatekeeper mutation was sufficient to abrogate the inhibitory effect of ZD6474 on MET uptake. There was a consistent increase in MET uptake in the H1975-VEGFR2^{V916M} tumors irrespective of ZD6474 treatment as detected by PET over a time span of two weeks.

Fig. S2A (left panel): Compound screening for S6K phosphorylation in H1975, H441 and HCC1359

Cell lines were pretreated for 4 hours with the indicated compounds (Z= ZD6474 1 μ M, Rapa= Rapamycin 0.1 μ M, PIK90 0.2 μ M, PTK787 10 μ M and 20 μ M, Torin1 0.25 μ M) and then stimulated with 40ng VEGF (V) for 30 minutes. Cell lysates were prepared and immunoblotted with the indicated phospho-specific antibody. The blots revealed that all the compounds including VEGFR2 inhibitor PTK787 were potent as inhibitors of S6K phosphorylation.

Fig. S2A (right panel): PDK1 as an alternative route for mTOR activation

H441 and H1975 cells were stimulated with 40ng VEGF (V) alone or in addition to pretreatment with ZD6474 (Z) 1 μ M. Impact on activation of downstream signaling via PDK1 was determined by immunoblotting, employing the indicated phospho-specific antibody:

Fig. S2B: Compound screening for VEGF secretion in H1975, H441 and HCC1359

Cells were plated in 6-well plates and incubated for 24 hours in starving media. Cells were then either stimulated with DMSO or 40 ng VEGF (V) alone or in addition to pretreatment with the Z= ZD6474 1 μ M, Rapa-Rapamycin 0.1 μ M, PIK90 0.2 μ M, PTK787 20 μ M, Torin1 0.25 μ M for 4 hours. Secretion of VEGF into cell culture supernatants was measured by VEGF Human ELISA Kit from Tebu-Bio GmbH (cat. No. ELH-VEGF-001) according to manufacturer's instructions. VEGF secretion was reduced under treatment with each compound.

Fig. S2C. VEGF is equally expressed in the supernatant and intracellularly

Cells were either stimulated with 40 ng VEGF (V) alone or in addition to pretreatment with ZD6474 (Z) 1 μ M. VEGF levels (both intracellular and supernatant) were elevated under VEGF stimulation and lessened under ZD6474 treatment in HCC1359 (high VEGFR2 expressing cell line). However, in H1650 and A549 (low VEGFR2 expressing cell lines) VEGF levels were minimally elevated under exogenous VEGF stimulation and uninhibited under ZD6474 treatment.

Fig. S2D. VEGF detected in ELISA is not due to remaining exogenous VEGF

Tumor cells were treated with VEGF and washed 3 times; new starving media was added and the media was harvested after 5 min. VEGF levels detected by ELISA remained unaltered by short-term VEGF stimulation. Thus, any exogenous VEGF added to the cells was almost completely removed after washing with PBS.

Fig. S3A,B: VEGF:VEGFR2 feed forward loop is a feature of high VEGFR2 expressing cell line.

HCC1359 and H1650, with high and low VEGFR2 expression levels respectively, were pretreated with ZD6474 (Z) 0.5 and 1 μ M for 4 hours and then stimulated with 40ng VEGF (V) for 30 minutes. Cell lysates were prepared and immunoblotted with the indicated phospho-specific antibodies. In HCC1359 pS6 was induced under VEGF stimulation, which coincided with reduced pERK levels (A). Inhibition of VEGFR2 blunted pS6 and induced pERK (A). However, none of these effects was observed in H1650 (B).

Fig. S3C: VEGF:VEGFR2 autocrine signaling is also active in the physiological response to hypoxia

2x10⁶ cells of H1975 and H441 were plated in 6-well plates and incubated for 48 hours under hypoxia (16% and 1% O₂) in starving media containing either DMSO (D) alone or in combination with the ZD6474 (ZD) 1 μ M. Secretion of VEGF into cell culture supernatants was measured by VEGF Human ELISA Kit from Tebu-Bio GmbH (cat. No. ELH-VEGF-001) according to manufacturer's instructions.

Fig. S3D,E: VEGF:VEGFR2 feed-forward signaling cascade is active only under VEGF-induced phosphorylation.

H441 and H1975 were treated with D=DMSO; Z= ZD6474 1 μ M, Rapa-Rapamycin 0.1 μ M, and PIK90 0.2 μ M for 4 hours and either tested for VEGF secretion by ELISA (D) or immunoblotted for specific pharmacodynamic markers (E). There was minimal or almost no inhibitory effect on VEGF secretion. ZD6474 alone had no inhibitory effect on pS6 or pERK levels in both cell lines.

Fig. S4: See supplementary note

Fig. S5A: VEGFR2 knockdown does not affect cell proliferation

H1975 (KD, EV and WT) were cultured over time and quantified. No difference in cell-count was detected between the three cell lines.

Fig. S5B: VEGFR2 knockdown in tumor cells almost entirely abrogates initiation of tumor growth in vivo

H441^{wt} cells were stably transduced with lentiviral shRNA vectors targeting VEGFR2 or with empty vector control (eV). Knockdown efficiency was determined by western blotting, with wild-type as control. (upper panel). Knockdown, empty vector and wildtype H441 cells were engrafted subcutaneously in nude mice and tumor growth were monitored over time. (lower panel):

Fig. S5C: Silencing of VEGFR2 dramatically reduces secretion of VEGF in tumor cells irrespective of HIF-1alpha levels.

H1975^{ev} tumors engrafted in nude mice were explanted on day 6 when they were approximately the same size as H1975^{VEGFR2 KD} tumors ($\approx 100\text{mm}^3$). Tumors were explanted and flash-frozen in liquid nitrogen. They were then lysed with a homogenizer in organ lysis buffer (800 μ l/tumor) and stained for HIF-1alpha by immunoblotting. HIF1alpha stainings of Jurkat and H1975-NSCLC cells were performed under hypoxic (1% O₂) and normoxic (16% O₂) in vitro conditions. Jurkat cells were used as positive control for HIF1alpha staining. HIF-1alpha expression was not completely blunted by VEGFR2 KD. Staining of VEGF was performed by immunohistochemistry.

The data indicated that even if there was a massive difference in VEGF expression levels between KD and EV tumors, HIF-1alpha levels remained quite constant in all cell types.

Fig. S5D: Stable cell lines were injected into nude mice and uptake of ¹¹⁰O-labeled H₂O was determined by PET.

Blots indicate percentage change in tumor blood flow as detected by 110-H₂O PET.

Fig. S5E: Low VEGFR2 expressing tumor cell lines are unaffected by VEGFR2 inhibition

H1650 [EGFR^{mut}] and A549 [KRAS^{mut}] with low expression of VEGFR2 were selected. 5x10⁶ cells from each cell line were implanted subcutaneously in mice. Treatment was started on day 1 after injection of the tumor cells. Tumors were treated daily with an oral gavage of 75mg/kg ZD6474 or vehicle and tumor volumes were recorded over time.

Fig. S5F: VEGF: VEGFR2 feed-forward loop inhibition leads to reduction in vessel density

H1975^{WT} tumors were explanted from mice treated daily with an oral gavage of 75mg/kg ZD6474 or vehicle for 2 weeks and were imaged for microvessels under a phase-contrast inverted-light microscope (Axiovert 135, Zeiss, LLC, US) with 40X magnification.

Fig. S6: Activation of the autocrine VEGF:VEGFR2 signaling loop is a feature of highly angiogenic lung adenocarcinomas.

Immunohistochemical stainings of VEGF and VEGFR2 in 117 surgically resected primary human lung adenocarcinomas revealed that VEGF expression correlated significantly with expression of VEGFR2 on the same tumor cells ($p=2.612 \times 10^{-5}$) as well as with microvessel density ($p=2.2 \times 10^{-11}$). Four examples are shown where row 0 represents low VEGF expression correlating with low VEGFR2 expression and almost no microvessels (CD31 staining). Row 1 represents a moderate VEGF:VEGFR2:CD31 expression co-relation where as rows 3 and 4 indicate very high VEGF:VEGFR2 expression levels associated with increasing microvessel density.

Fig. S7A,B: High VEGFR2 expressing tumors are sensitive to combined inhibition of VEGFR2 and ERK signaling

Apart from H1975, we also engrafted H441 and HCC1359 (both with high VEGFR2 expression levels) subcutaneously in nude mice and recorded tumor volumes over time under treatment with either vehicle or ZD6474 (75mg/kg) alone, PD0325901 (12mg/kg) alone, or combined PD0325901 plus ZD6474.

Fig. S7C,D: Low VEGFR2 expressing tumors are insensitive to combined inhibition of VEGFR2 and ERK signaling

Sizes of subcutaneously grown H1650 and A549 tumors were determined at the indicated time points under treatment with either vehicle or ZD6474 (75mg/kg) alone, PD0325901 (12mg/kg) alone, or combined PD0325901 plus ZD6474.

Fig. S7E,F: ZD6474 treatment decreases phosphorylation of S6 and induces phosphorylation of pERK in high VEGFR2 expressing NSCLC in vivo

After treating mice over a timespan of 28 days, either with vehicle or ZD6474 (75mg/kg daily with oral gavage), tumors were explanted and lysed for immunoblotting. pS6 levels were reduced under Zactima treatment compared to vehicle in H1975, H441 and in HCC1359 tumors (E). Inhibition of VEGFR2 simultaneously induced pERK (E). However, none of these effects was observed in H1650 or in A549 tumors (F).

Fig. S7G: Combined ZD6474 and PD0325901 treatment decreases phosphorylation of ERK

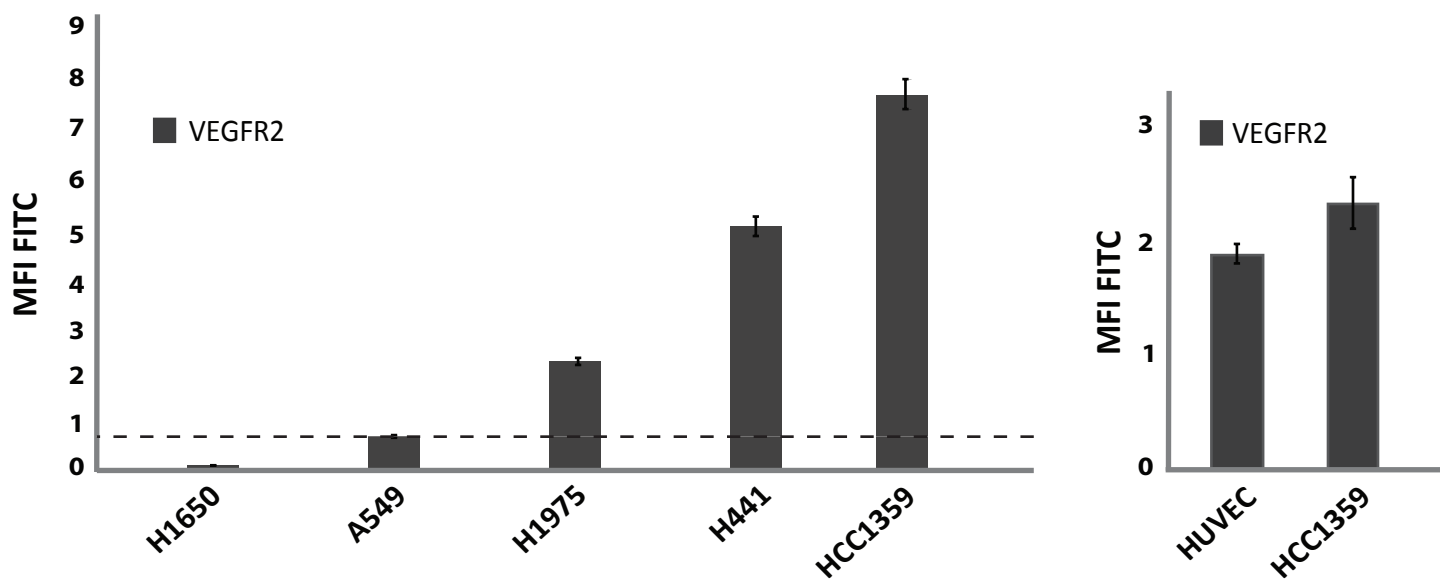
The impact of combined ZD6474 and PD0325901 treatment on IRS1, pERK and pAKT was determined by western blots employing the indicated antibodies. Combined treatment resulted in inhibition of pERK.

Fig. S7H: VEGFR2 expression on the tumor cells of the murine Ras-mutated lung cancer model

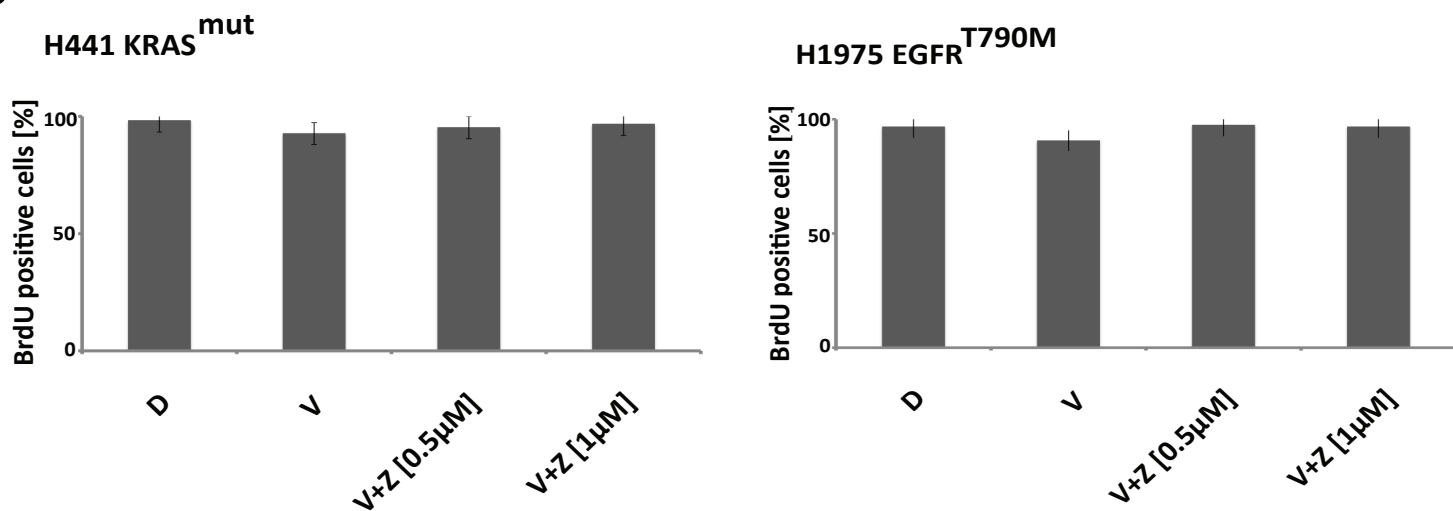
Murine lung tumors were stained with antibodies recognizing human VEGFR2. Murine Ras-mutated lung tumor cells were positive for VEGFR2.

Figure S1

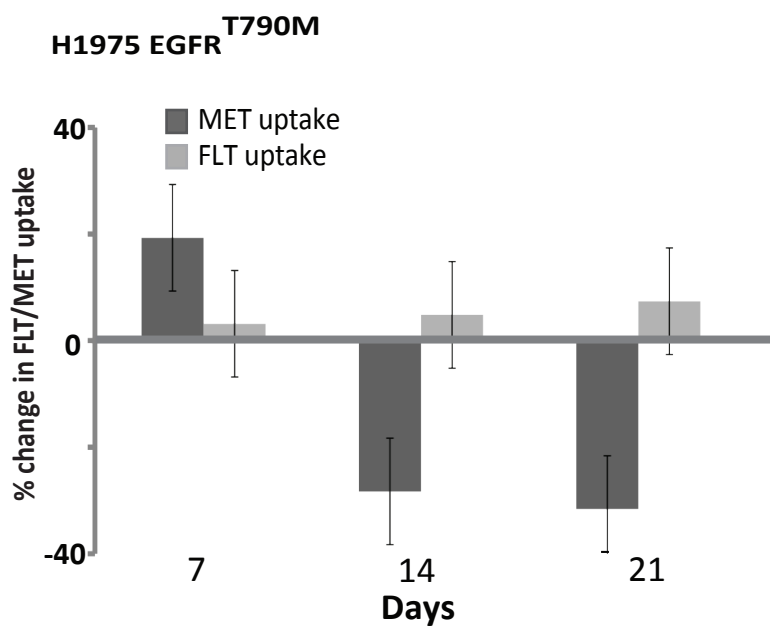
A



B



C



D

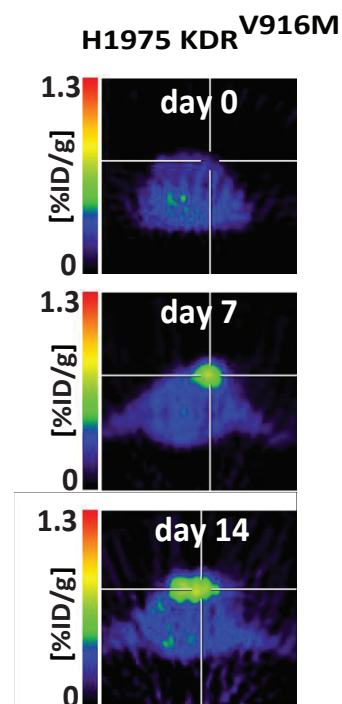
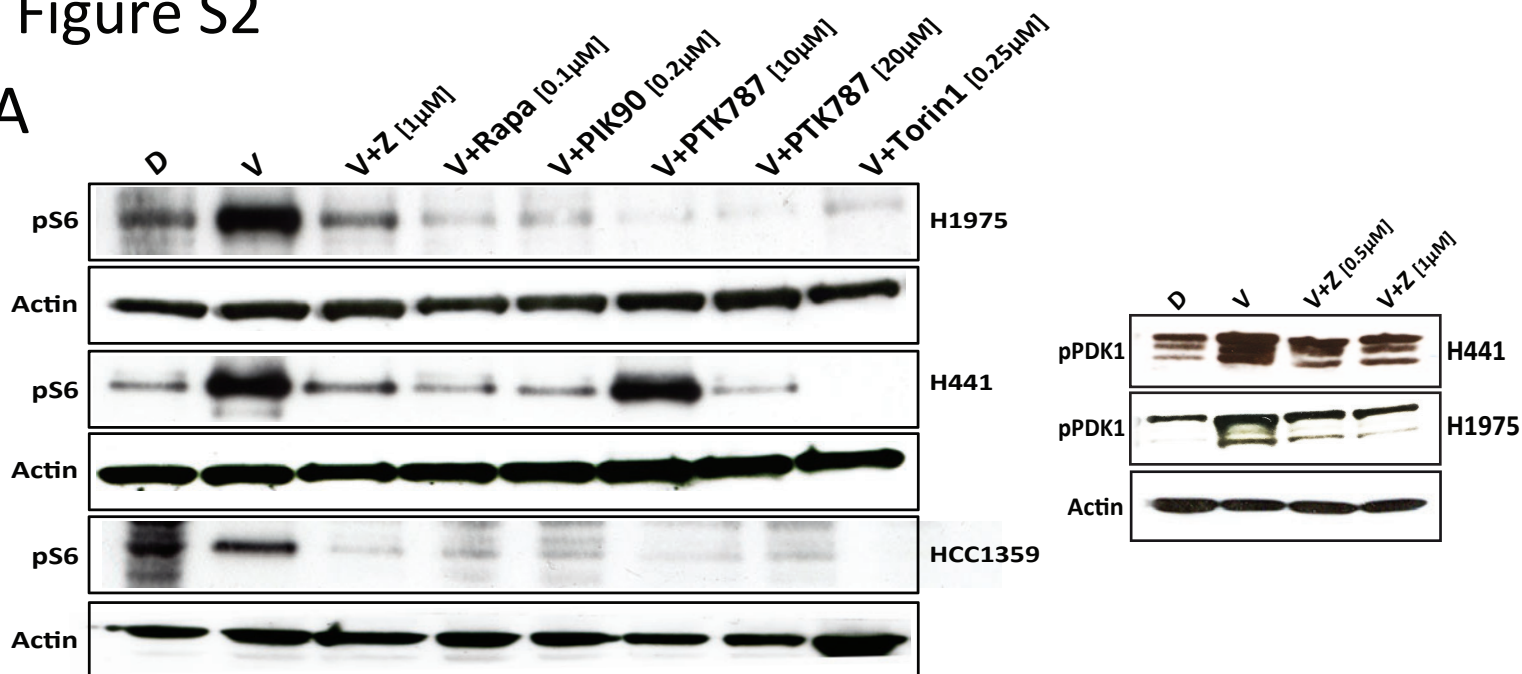
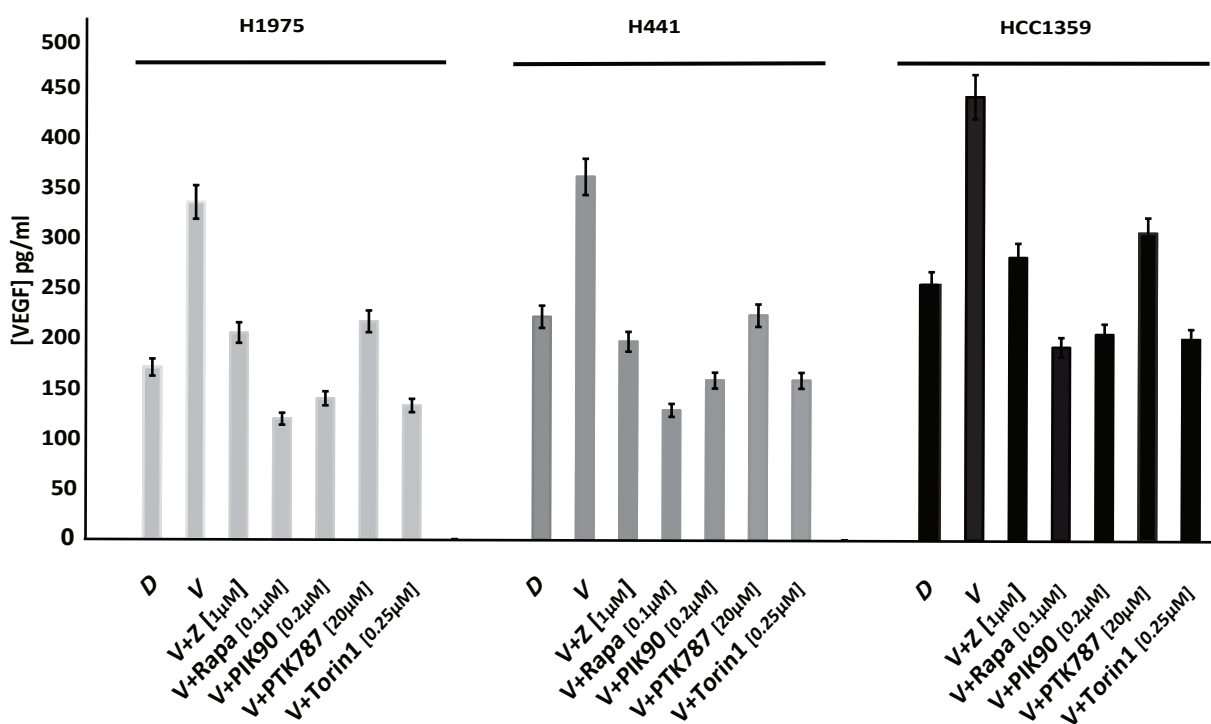


Figure S2

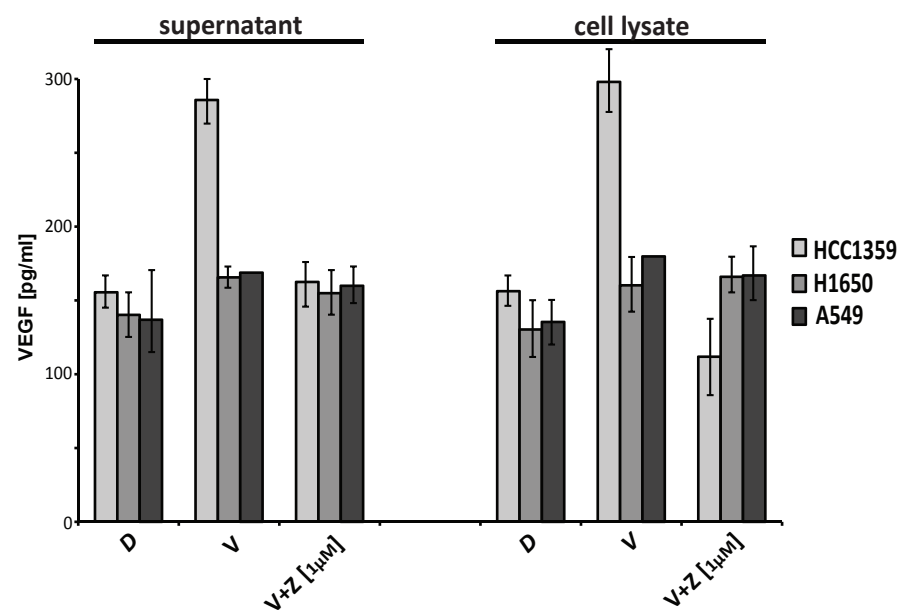
A



B



C



D

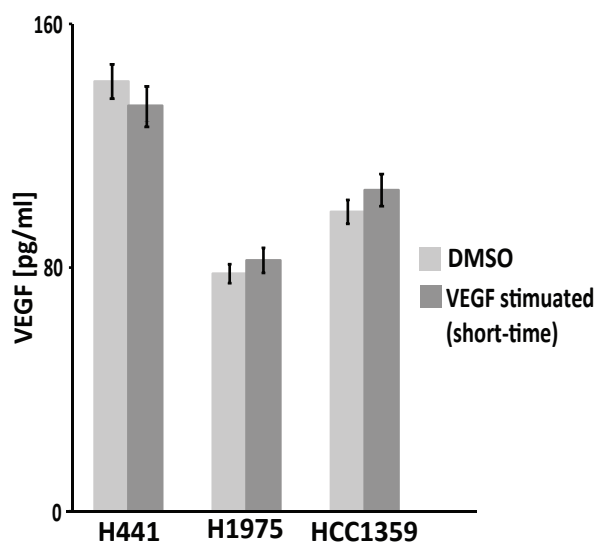
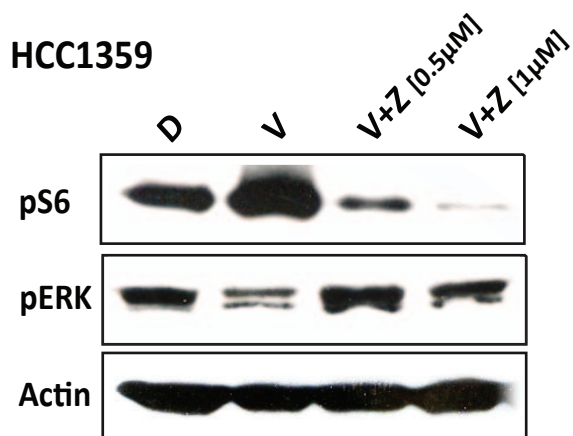
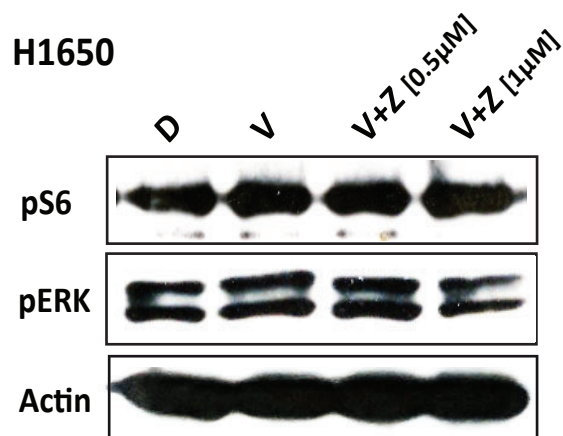


Figure S3

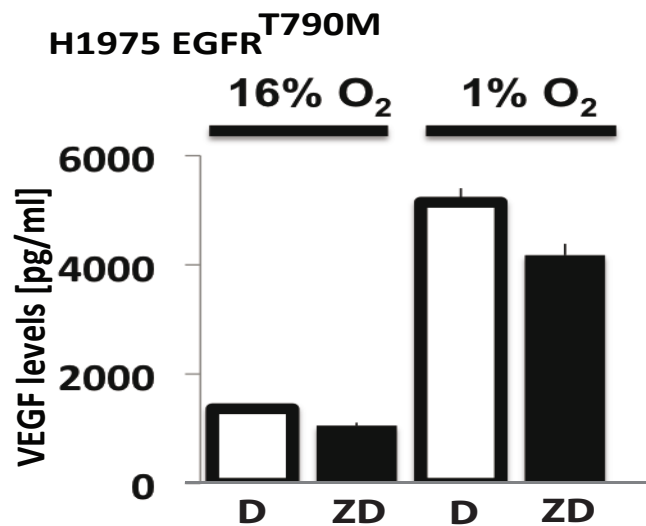
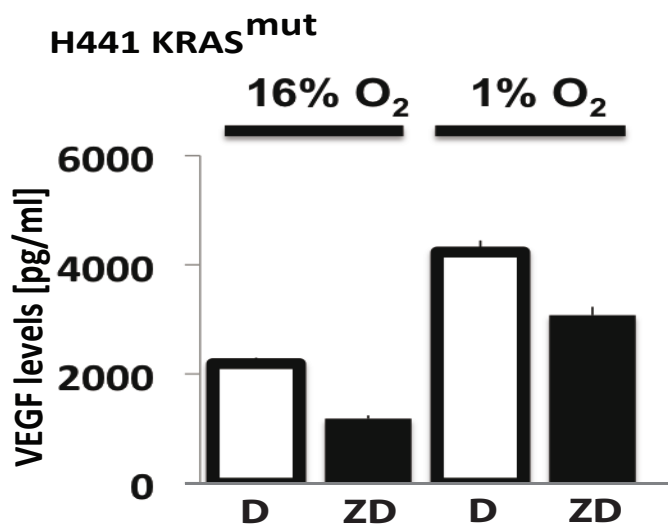
A



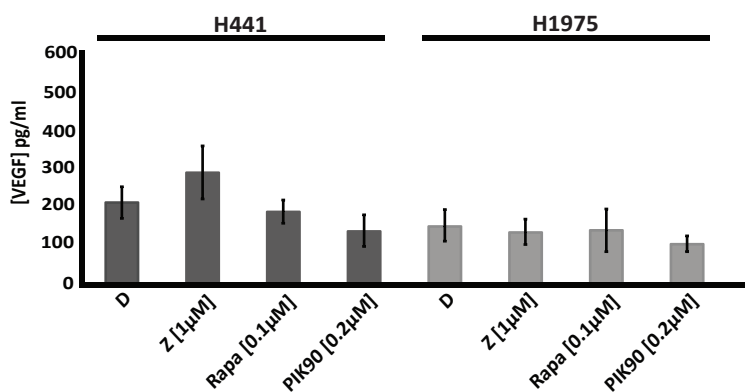
B



C



D



E

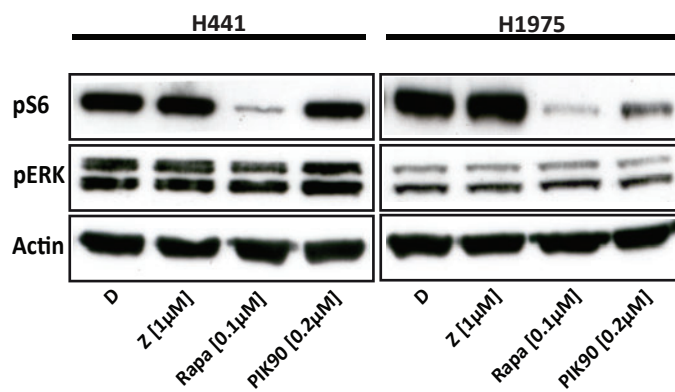
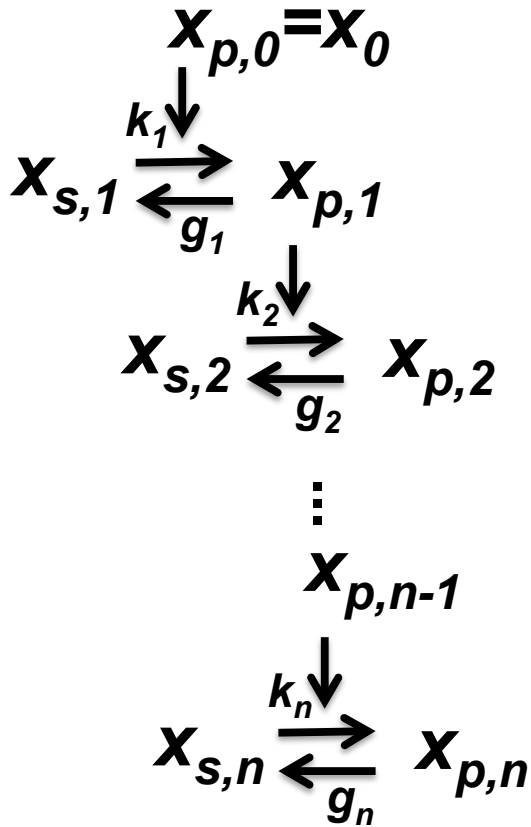
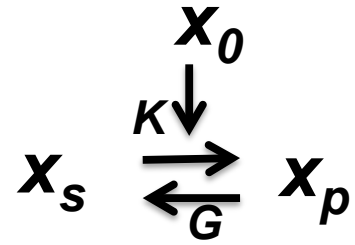


Figure S4

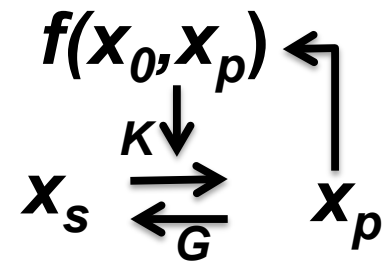
A



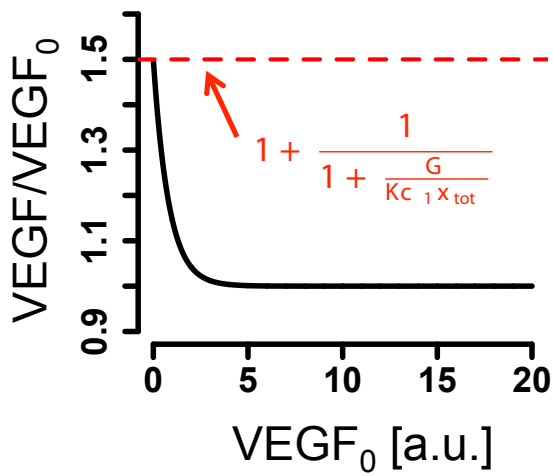
B



C



D



E

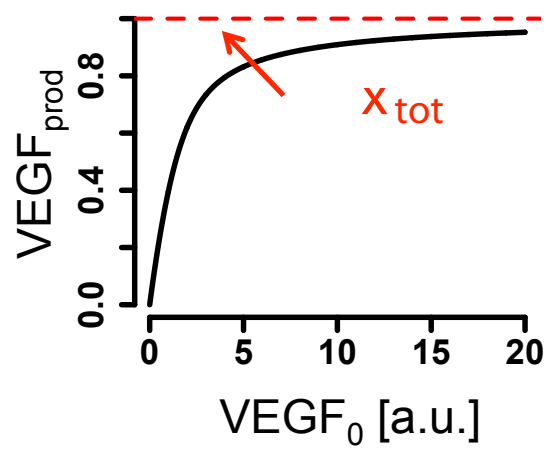
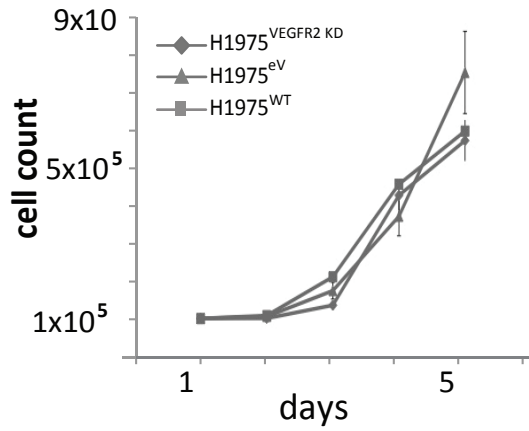
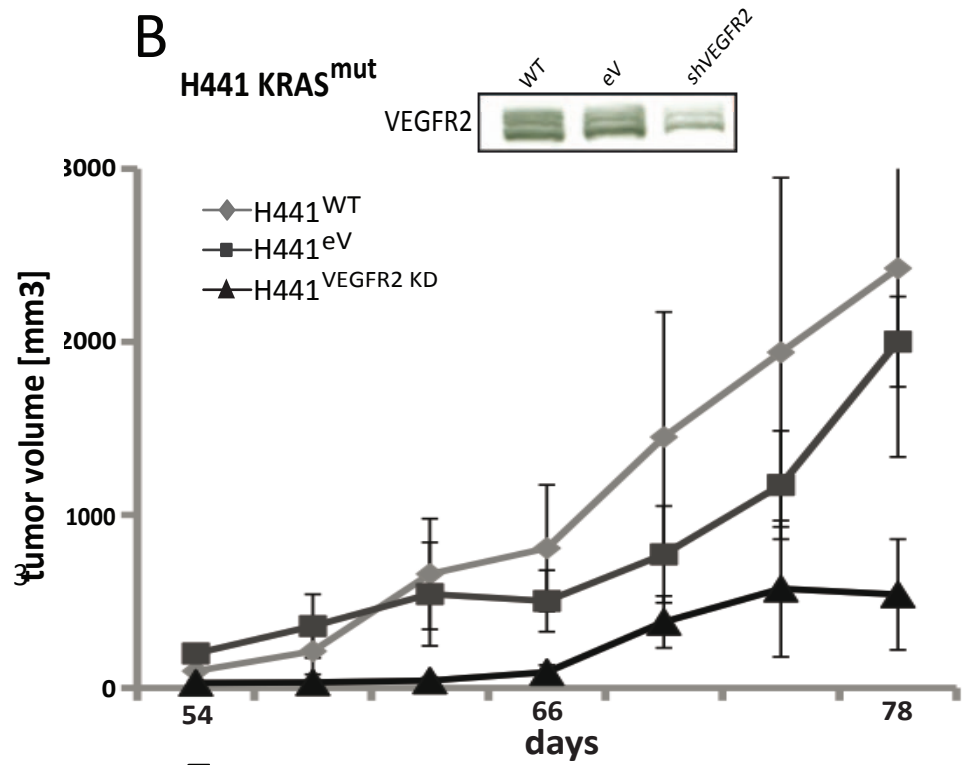


Figure S5

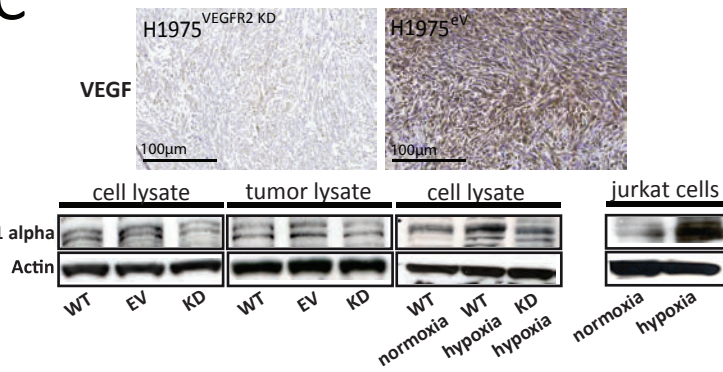
A



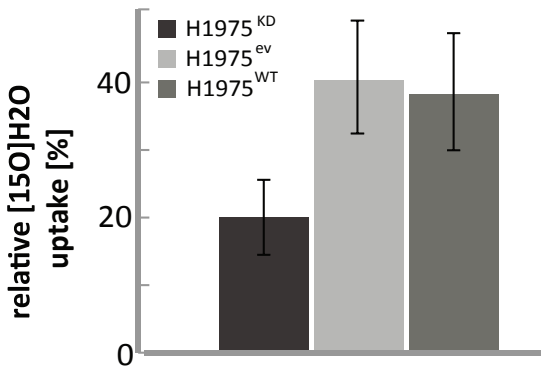
B



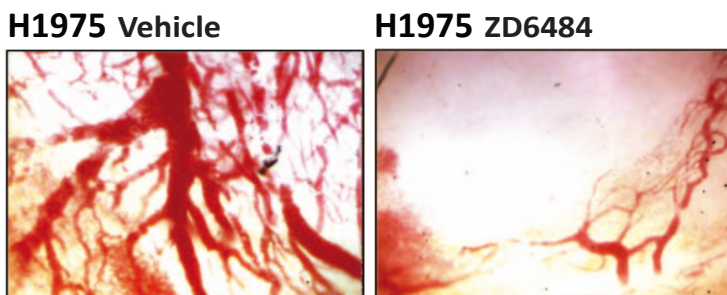
C



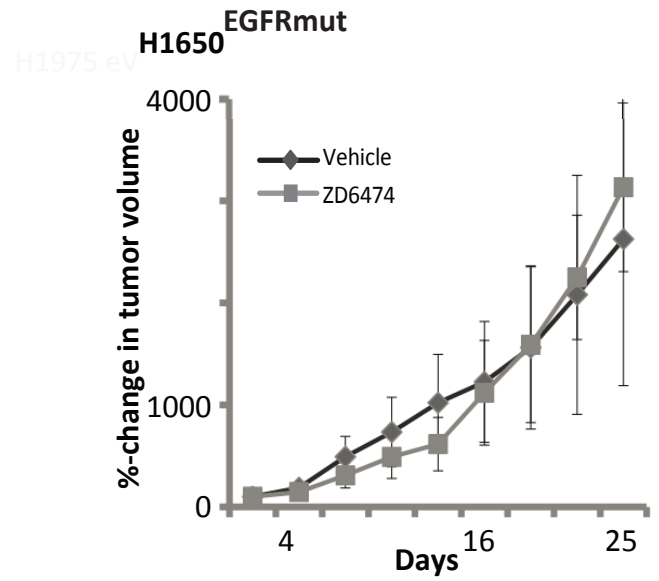
D



F



E



A549 KRASmut

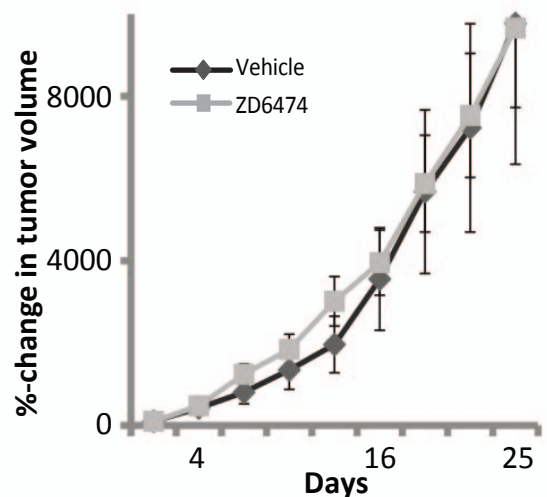


Figure S6

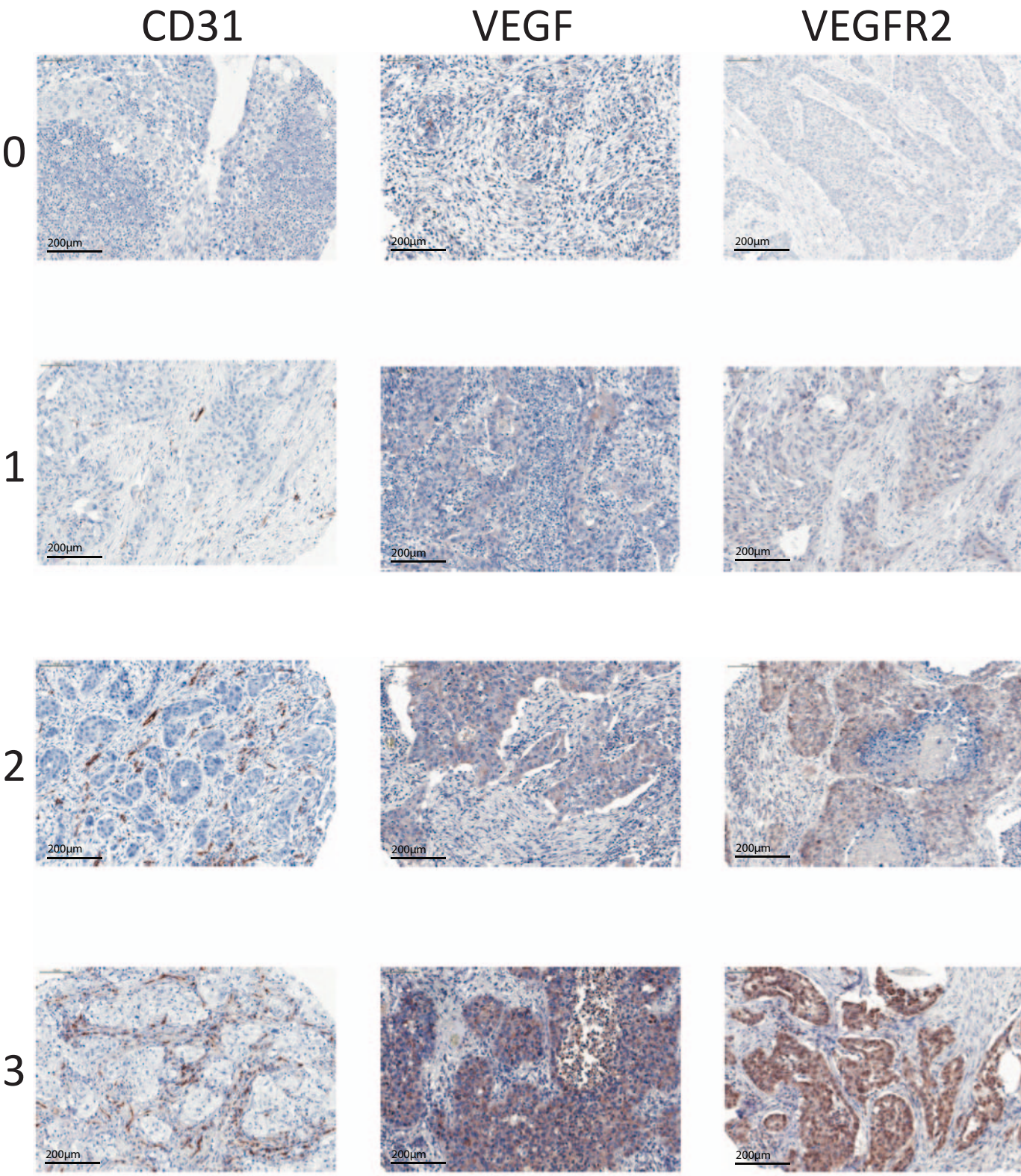
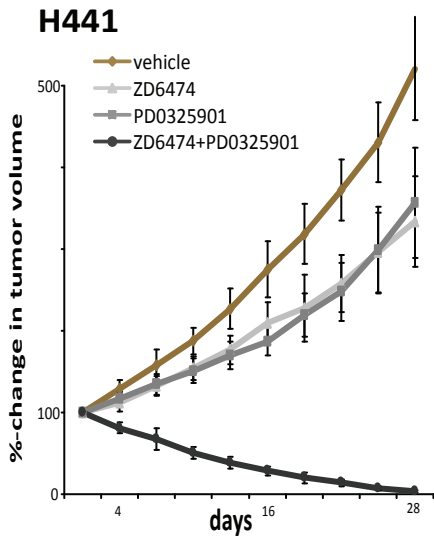
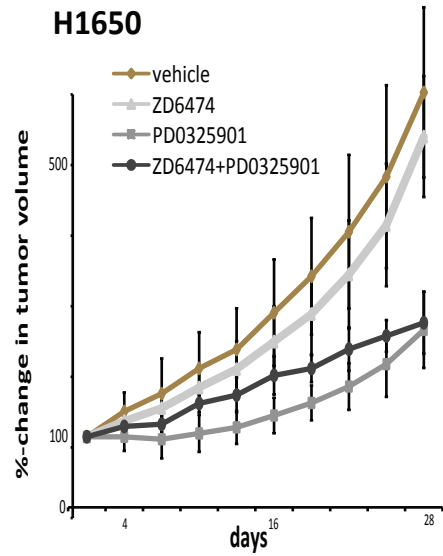


Figure 7

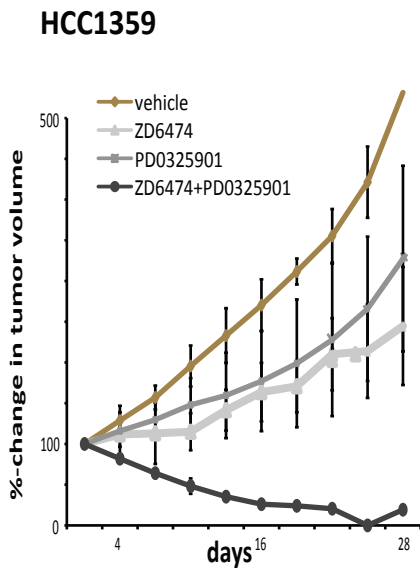
A



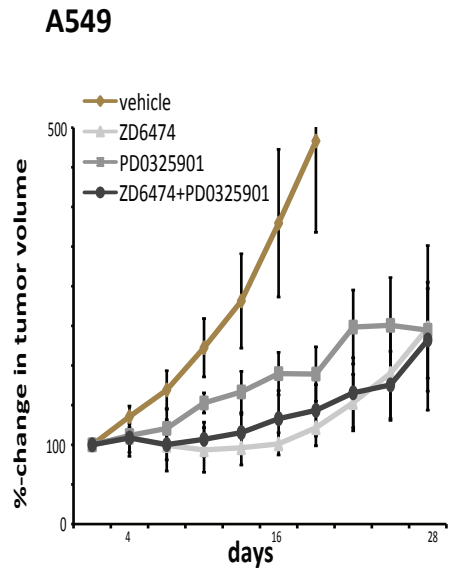
C



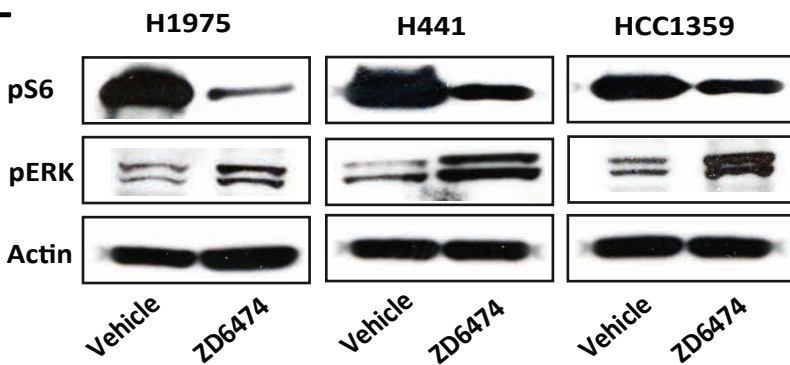
B



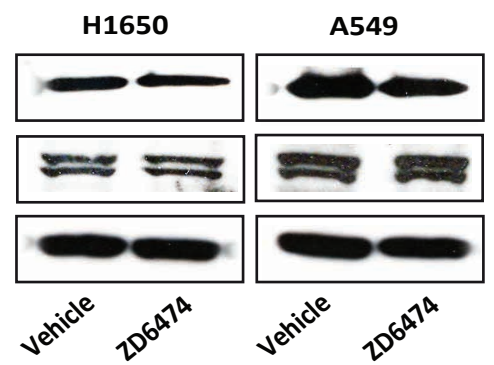
D



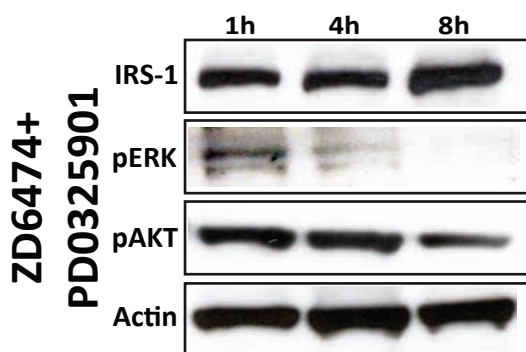
E



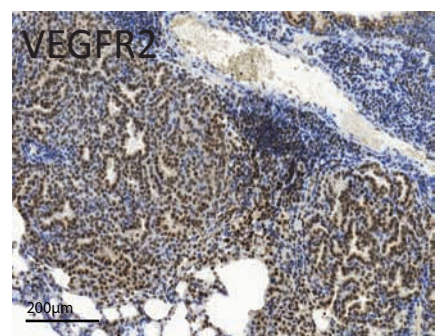
F



G



H



Supplementary Note

A mathematical model describing the VEGF-VEGFR2 feedforward mechanism in tumor cells

The general model without positive feedforward loop

First, we formulate a simple model describing a signaling cascade, where each protein is activated by the previous step. The network of this signaling cascade involving n reactions is shown in **Fig. S3A**. Here, $x_{s,i}$ is the concentration of protein $i \in \{1, \dots, n\}$ in its inactivated form and the concentration of the corresponding activated form is $x_{p,i}$. Kinetic parameters of the forward reaction are represented by k_i and for the backward reaction by g_i respectively. For the sake of simplicity, the concentration of the input x_0 is denoted as $x_{p,0}$. By the law of mass action, the dynamics of each reaction is modeled by the following set of two ordinary differential equations:

$$\begin{aligned}\frac{dx_{s,i}}{dt} &= -k_i x_{p,i-1} x_{s,i} + g_i x_{p,i} \\ \frac{dx_{p,i}}{dt} &= +k_i x_{p,i-1} x_{s,i} - g_i x_{p,i}.\end{aligned}\tag{S1}$$

Let $x_{tot,i}$ be the total concentration of protein i . By conservation of total mass $x_{s,i} + x_{p,i} = x_{tot,i}$ is constant in time. Thus, we can substitute $x_{s,i} = x_{tot,i} - x_{p,i}$ in Eq. (S1) such that the system is fully characterized by

$$\frac{dx_{p,i}}{dt} = k_i x_{p,i-1} (x_{tot,i} - x_{p,i}) - g_i x_{p,i}.\tag{S2}$$

We next show that the equilibrium of the full system can be equivalently described by a single-step reaction network ($n=1$). To this end, we determine the equilibrium of each sub-reaction by setting the derivative in Eq. (S2) to zero. This yields

$$x_{p,i}^* = \frac{x_{tot,i}}{1 + \frac{g_n}{k_n x_{p,i-1}^*}},\tag{S3}$$

where $x_{p,i}^*$ denotes the equilibrium value of $x_{p,i}$ for all $i \in \{1, \dots, n\}$. Inserting the expression of $x_{p,n-1}^*$ as given by Eq. (S3) into the expression of $x_{p,n}^*$, we obtain after straightforward algebraic manipulations

$$x_{p,n}^* = \frac{x_{tot,n} \left(1 + \frac{g_n}{k_n x_{tot,n-1}}\right)^{-1}}{1 + \frac{g_n g_{n-1} (k_n x_{tot,n-1} + g_n)}{x_{tot,n-1}^2 k_n^2 k_{n-1}} \frac{1}{x_{p,n-2}^*}}$$

By setting $K = x_{tot,n-1}^2 k_n^2 k_{n-1}$, $G = g_n g_{n-1} (k_n x_{tot,n-1} + g_n)$, and $x_{tot} = x_{tot,n} \left(1 + \frac{g_n}{k_n x_{tot,n-1}}\right)^{-1}$ as effective parameters for the last step, we can reduce system to $n - 1$

reactions keeping the equilibrium value to that of n reactions. Inductively we can conclude that there are effective parameters K , G , and x_{tot} such that the equilibrium of a single-step model (**Fig. S3B**) is equal to that of the n reaction model (**Fig. S3A**). The differential equation of this reduced model yields

$$\frac{dx_p}{dt} = Kx_0(x_{tot} - x_p) - Gx_p. \quad (\text{S4})$$

It should be noted that unless the equilibrium is equal to the full n -step model, the overall dynamics may slightly differ. Since we are mainly interested in the change of the equilibrium value if a positive feedforward is added, we are restricted the following discussion to the one step model.

Adding the positive feedforward loop to the model

The feedforward loop is added to the single-step model, Eq. (S4), by replacing the input x_0 with $f(x_0, x_p)$ (**Fig. S3C**), where the function f describes the mixing of the external protein concentration x_0 with that of the one produced (proportional to x_p). In the case of the proposed VEGF-VEGFR2 feedforward mechanism, $f(x_0, x_p)$ is the VEGF concentration in the medium and x_0 is the initial VEGF concentration. Thus, the system is represented by the one-dimensional differential equation

$$\frac{dx_p}{dt} = Kf(x_0, x_p)(x_{tot} - x_p) - Gx_p. \quad (\text{S5})$$

To further specify the unknown function f , we examine two extreme cases: $x_0 \ll x_p$ and $x_0 \gg x_p$. In the case of $x_0 \ll x_p$, the external VEGF concentration is much lower than the one produced, leading to an almost additive total concentration of the mixture: $f(x_0, x_p) \approx x_0 + c_1x_p$. At the opposite extreme $x_0 \gg x_p$, the produced VEGF has to be transported against a high osmotic pressure of the surrounding so that we would expect the VEGF produced to make a vanishing contribution: $f(x_0, x_p) \approx x_0$. In order to proceed with our analysis, we assume the following relationship in concordance with the extreme cases discussed above:

$$f(x_0, x_p) = x_0 + c_1x_p e^{-c_2x_0}, \quad (\text{S6})$$

where c_1 and c_2 are positive constants. Inserting Eq. (S6) into Eq. (S5) and computing the equilibrium value ($\frac{dx_p}{dt} = 0$) yields

$$x_p^* = \frac{1}{2Z(x_0)} \left[- \left(x_0 + \frac{G}{K} + Z(x_0)x_{tot} \right) + \sqrt{\left(x_0 + \frac{G}{K} + Z(x_0)x_{tot} \right)^2 + 4Z(x_0)x_0x_{tot}} \right],$$

where $Z(x_0) = c_1 e^{-c_2 x_0}$. The total concentration in the surrounding is therefore

$$f(x_0, x_p^*) = x_0 + \frac{1}{2} \left[- \left(x_0 + \frac{G}{K} + Z(x_0)x_{tot} \right) + \sqrt{\left(x_0 + \frac{G}{K} + Z(x_0)x_{tot} \right)^2 + 4Z(x_0)x_0x_{tot}} \right]. \quad (\text{S7})$$

Next, we examine the ratio between the total $f(x_0, x_p^*)$ and the initial x_0 VEGF concentration in the equilibrium. Since the concentration of x_p is bounded by x_{tot} , we obtain in the limit $x_0 \rightarrow \infty$: $f(x_0, x_p^*)/x_0 \rightarrow 1$. Expanding $f(x_0, x_p^*)$ around x_0 yields the limit $x_0 \rightarrow 0$ of $f(x_0, x_p^*)/x_0$ as

$$\lim_{x_0 \rightarrow 0} f(x_0, x_p^*)/x_0 = 1 + \frac{1}{1 + \frac{G}{Kc_1x_{tot}}} \leq 2. \quad (\text{S8})$$

Setting $f(x_0, x_p^*) = VEGF$ (total VEGF concentration in the medium) and $x_0 = VGFR_0$ (initial VEGF stimulation) we obtain a decreasing curve for $VEGF/VEGF_0$, starting at the value given by Eq. (S8) and ending at one (**Fig. S3D**). Moreover, any disruption of the signaling cascade or the absence of the feedforward loop leads to $VEGF = VEGF_0$.

Finally, we examine the amount of VEGF produced by the tumor cells alone. Since this is proportional to x_p^* we set $VEGF_{prod} \propto x_p^*$. Because the pathway saturates at high input concentrations, the limit of $VEGF_{prod}$ in case $VEGF_0 \rightarrow \infty$ is proportional to x_{tot} (**Fig. S3E**). In conclusion, $VEGF_{prod}$ reaches a plateau with increasing input concentrations $VEGF_0$.